SI Appendix

(2 Tables and 19 Figures)

Filling the Eastern European gap in millennium-long temperature reconstructions

Ulf Büntgen et al.

Table S1. Combination of the tree-ring data subsets used, the tree-ring index calculation methods applied, and the individual and composite detrending techniques performed.

Esemble Hierarchy	Esemble Members
Data	Pooled Living / Pooled Historical / Combined Living and Historical
Indexing	Ratios without Power-Transformation / Residuals after Power-Transformation
Individual Detrending	100yr / 200yr / 300yr splines / Hugershoff / Negative Exponential
Composite Detrending	RCS + 10yr spline / RCS + 67yr spline

Table S2. Reconstructed positive (left) and negative (right) extreme years (°C) and their corresponding uncertainty ranges. Those positive extremes that occurred during the recent warming after 1960 are indicated in red. Note that 33 positive extremes and only 16 negative extremes exceeded the two standard deviation threshold.

Positive Extreme	Temp. Anomaly (°C wrt 1961-90)	Recon. Error (°C wrt 1961-90)		Negative Extreme	Temp. Anomaly (°C wrt 1961-90)	Recon. Error (°C wrt 1961-90)	
2011	2.906127	0.504364	4.254116	1248	-4.16060687	-5.11875646	-2.19603224
1986	2.204065	1.088662	3.068192	1837	-3.96431571	-4.65266063	-1.96356412
1982	2.175596	1.172994	3.000809	1836	-3.851047	-4.28276783	-1.86417558
1981	2.109546	1.004331	2.990702	1814	-3.76335268	-4.13388214	-1.59801642
2008	1.804921	-0.09198	2.946904	1751	-3.68720702	-4.51479234	-2.20980593
1969	1.531043	0.998307	2.266345	1507	-3.551926	-4.513375	-1.84396096
1970	1.456453	0.898916	2.170326	1832	-3.49332349	-3.92305277	-1.3588101
1596	1.15866	-0.01066	2.311828	1638	-3.45114348	-4.1248466	-1.66371394
2002	1.154105	-0.11005	2.091152	1786	-3.44450786	-4.25134422	-1.69066676
2000	1.137593	0.05861	2.104628	1637	-3.43477344	-3.88389875	-1.7622602
1979	1.113109	0.332689	1.910905	1361	-3.4175493	-4.23026128	-1.33522637
1589	1.064141	0.206191	1.904166	1794	-3.41262339	-4.09773996	-1.40111976
1983	0.99923	0.130895	1.8351	1813	-3.36946203	-3.61885612	-1.06599335
1757	0.995155	1.141291	1.929435	1811	-3.35885339	-3.73740758	-1.14824115
1998	0.989551	-0.07391	1.949649	1091	-3.32815464	-4.09773996	-1.81700813
1122	0.892754	-0.71543	2.726228	1265	-3.32758525	-4.28748639	-1.46830595
1961	0.864854	0.344736	1.594209				
1999	0.836953	-0.15222	1.764349				
1966	0.830121	0.010421	1.670014				
2009	0.788555	-1.02867	1.924381				
1575	0.781722	0.323653	1.875529				
1738	0.767743	0.667004	2.070937				
1971	0.726491	0.194144	1.469552				
2010	0.686064	-1.07083	1.826677				
1774	0.661315	0.893093	1.823308				
1964	0.65247	0.215227	1.467867				
1997	0.647346	-0.3751	1.622846				
1595	0.646776	-0.33594	1.671698				
1594	0.638235	-0.02271	1.654853				
1597	0.629125	-0.58894	1.877214				
1406	0.60578	0.453163	1.237084				
1748	0.593432	-0.11306	2.096494				
1712	0.591159	-0.04336	1.771087				

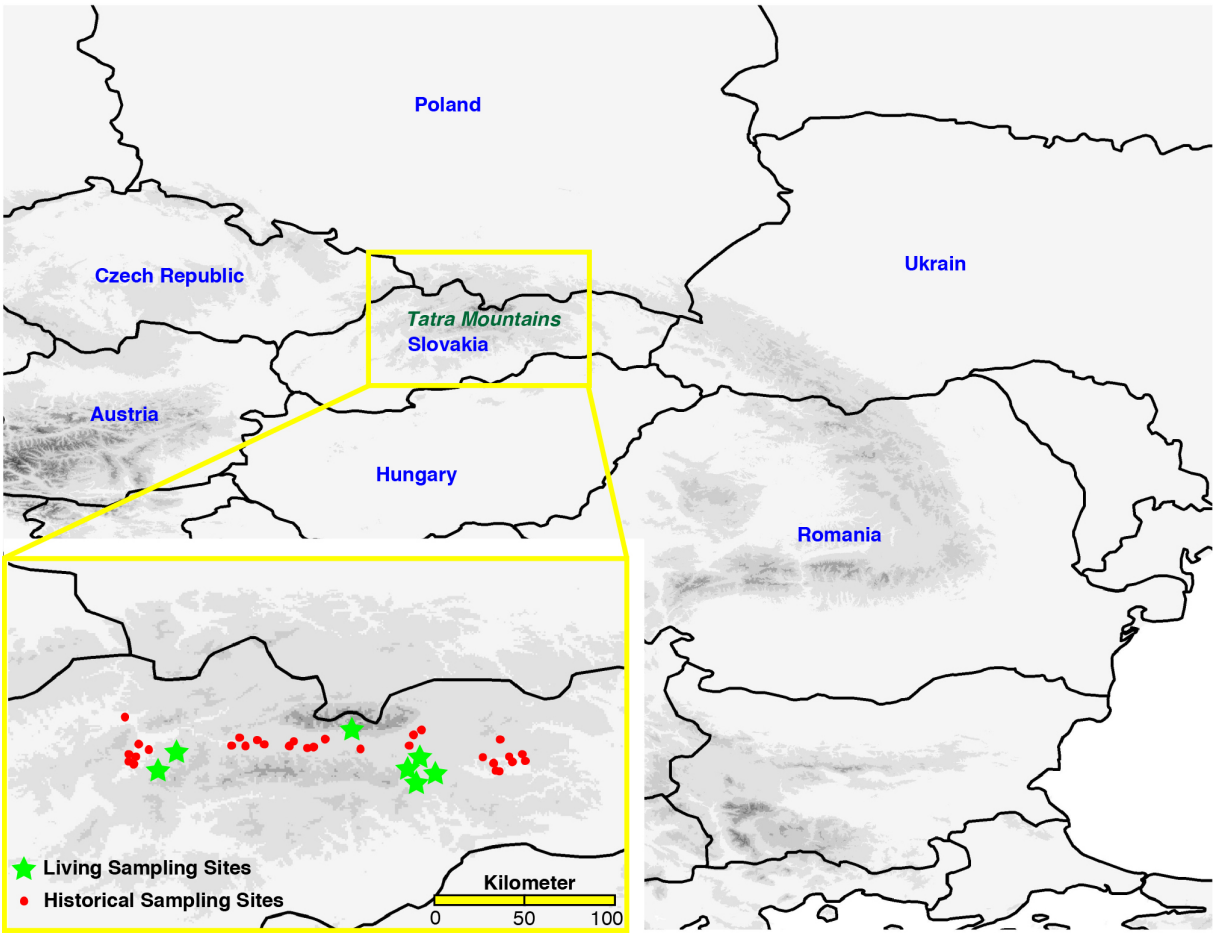

Fig. S1. Location of the living and historical sampling sites within the area of the Tatra Mountains in northern Slovakia.

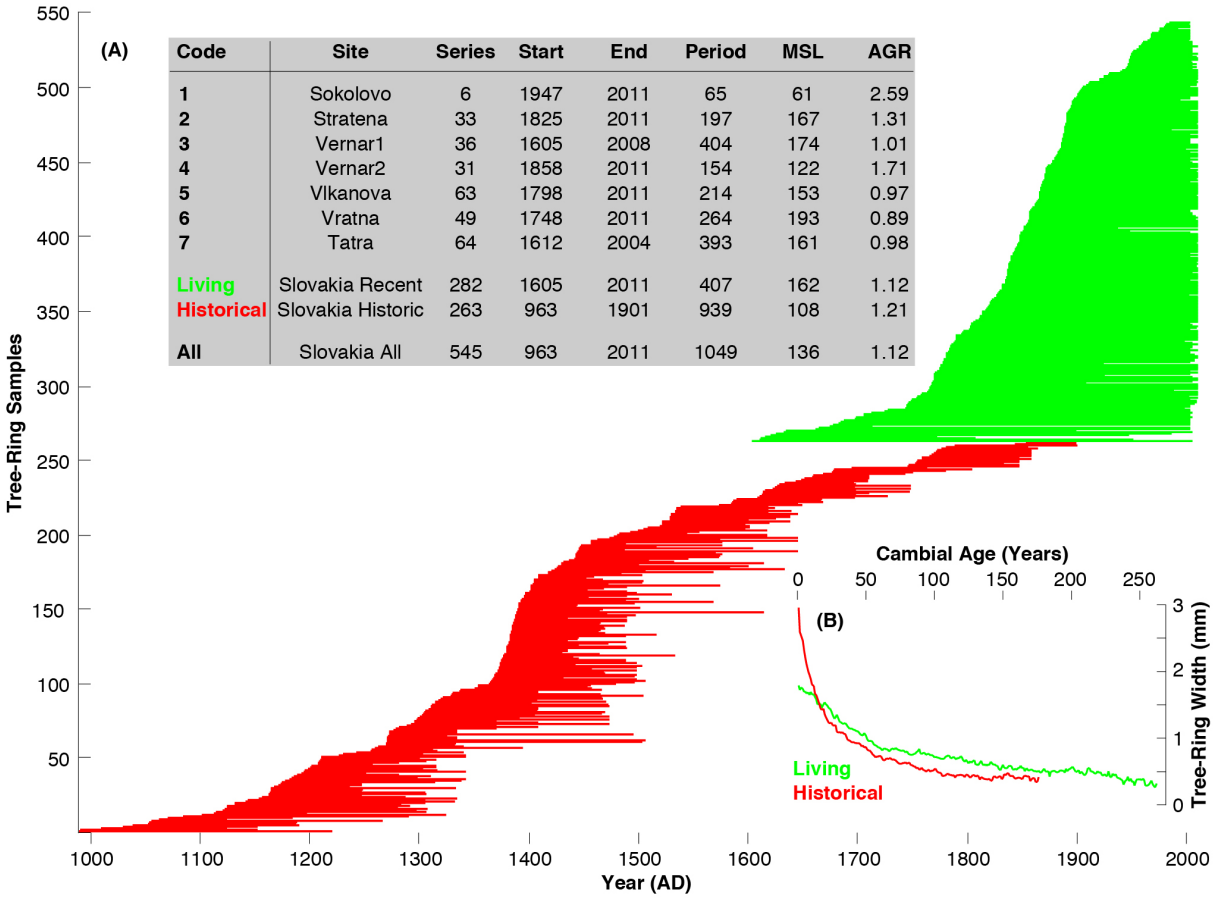

Fig. S2. (A) Temporal distribution of the 282 living and 263 historical samples between 963 and 2011 AD. The inset provides information of the seven individual living sampling sites, the historical subset and a combination thereof (All). Mean Segment Length (MSL; years) and Average Growth Rate (AGR; mm) refer to the raw measurement series without standardization. **(B)** Average growth trends of the living and historical subsets expressed by their Regional Curves (RCs) after age-aligning each individual measurement series by its cambial age.

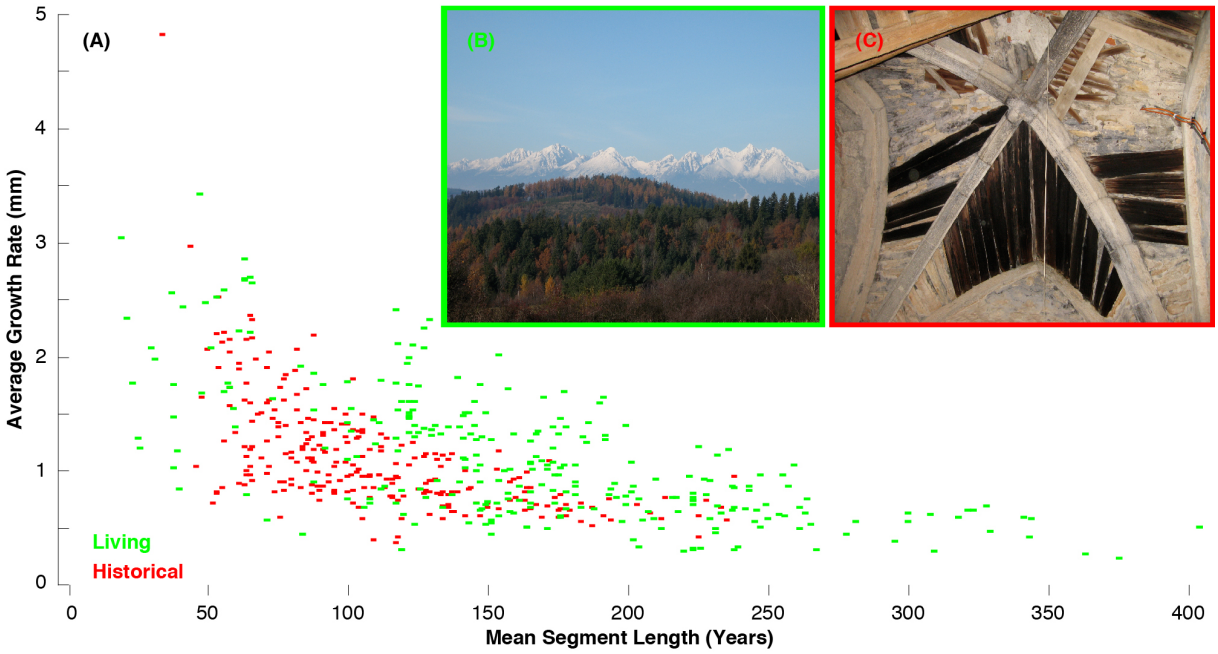

Fig. S3. (A) Relationship between Average Growth Rate (AGR; mm) and Mean Segment Length (MSL; years) of the 282 living and 263 historical samples. Digital images of **(B)** a typical mixed larch (*Larix decidua*) and spruce (*Picea abies*) forest stand (~900 m asl) in the northern Slovakian foothills of the High Tatra Mountains (in the background), and **(C)** larch construction wood from a vault in northern tower of St. Martin church in Spisské Podhradie, northern Slovakia.

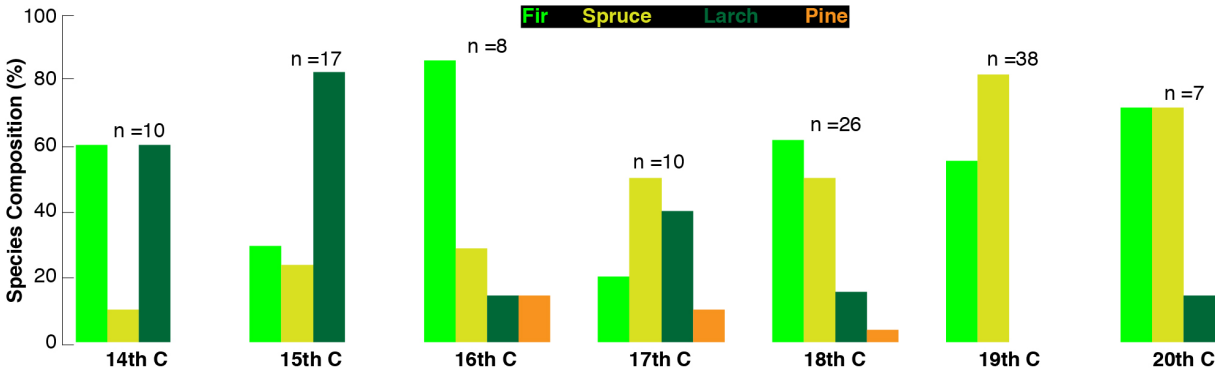

Fig. S4. Percentage of conifer species used as construction timber throughout the past seven centuries, with n referring to the absolute number of investigated roof constructions in northern Slovakia.

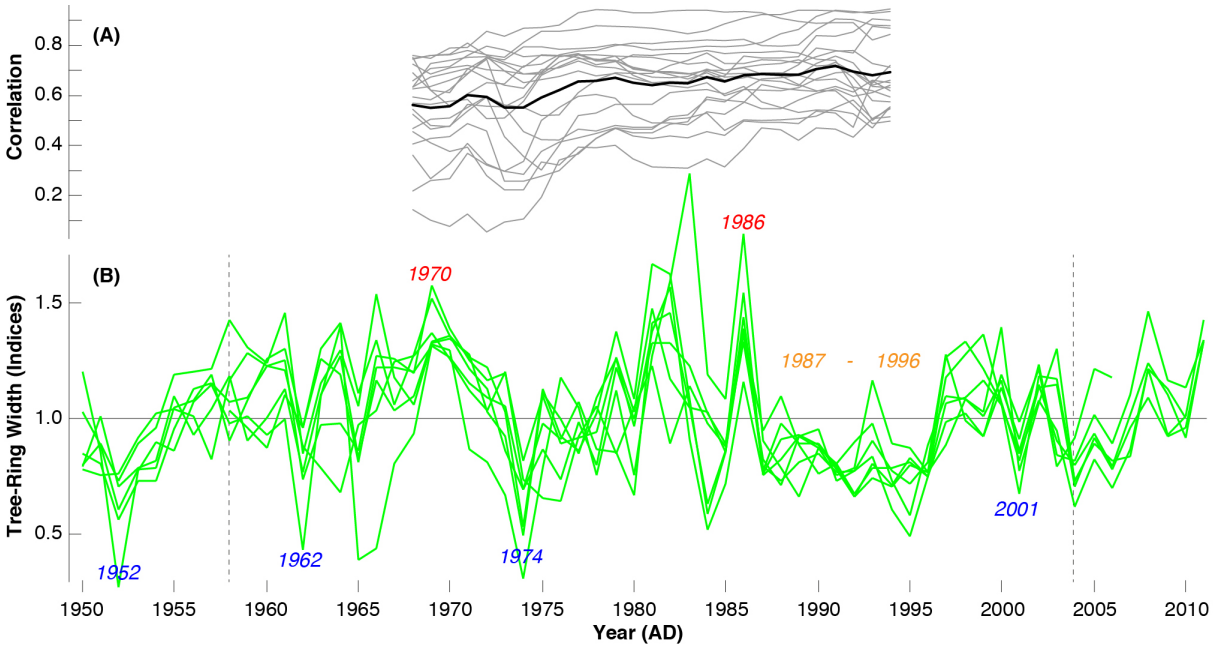

Fig. S5. (A) Moving 21yr cross-correlation coefficients between **(B)** seven living tree-ring width chronologies after 100yr spline detrending. The black line refers to the grand average correlation, and the common period of all seven records after truncation at <6 series is 1958-2004. Distinct growth anomalies are labeled.

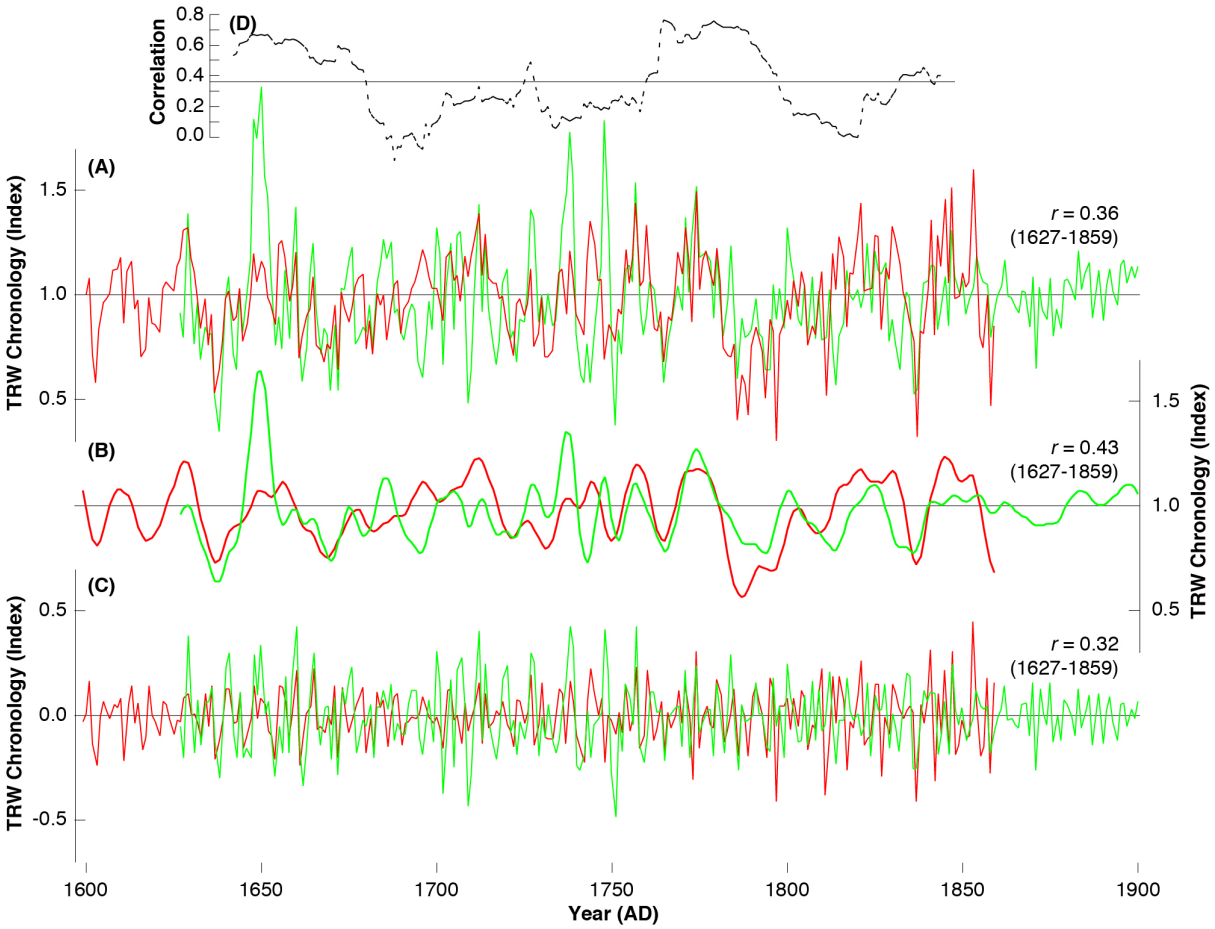

Fig. S6. (A) Comparison between the 1627-1859 overlapping period of the living (green) and historical (red) chronologies after truncation <6 series and individual 100yr spline detrending. **(B)** Decadal and **(C)** interannual variability of these chronologies after 10yr low- and high-pass filtering, respectively. **(D)** Moving 31yr correlation coefficients between the original unfiltered chronologies.

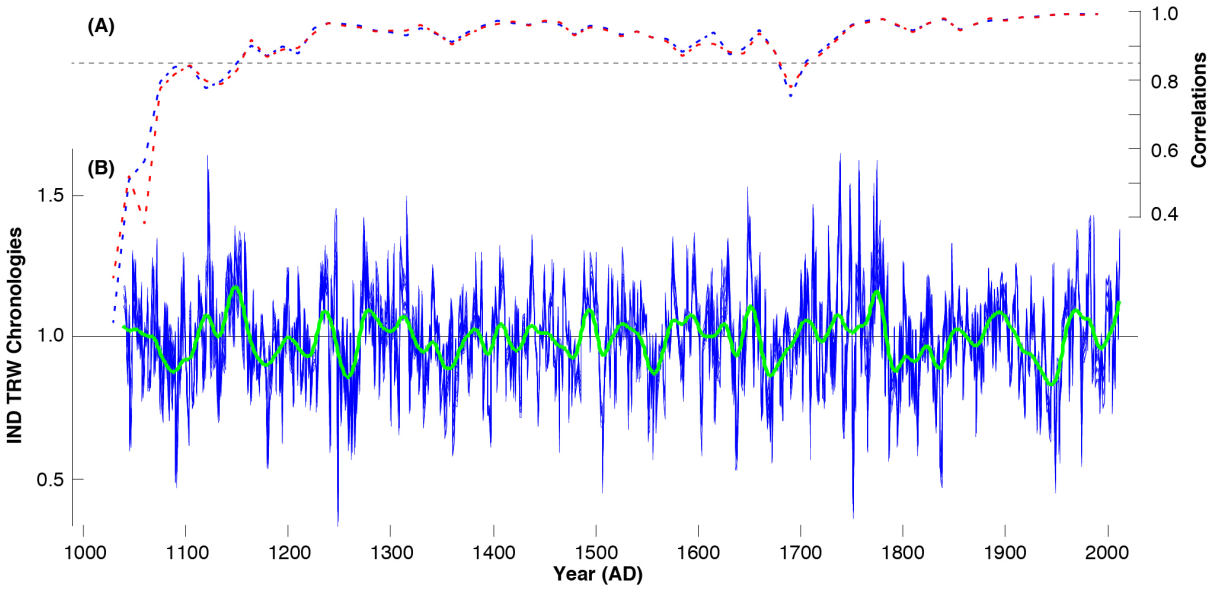

Fig. S7. (A) Temporal expression of the mean Expressed Population Signal (EPS; computed over 30-year windows lagged by 15 years) of **(B)** the 2 IND (blue) chronologies, with the green curve being a 40-year low-pass filter.

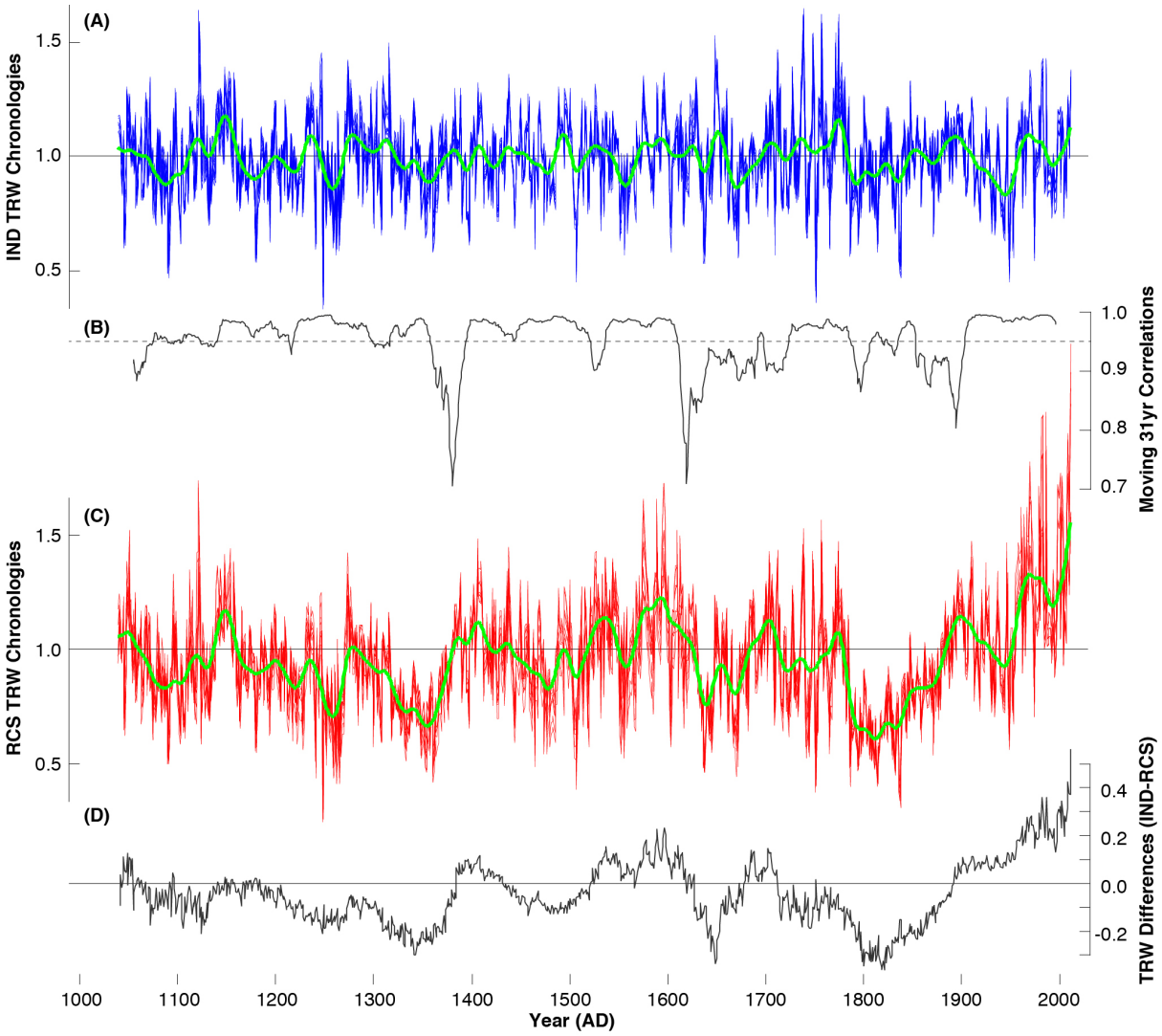

Fig. S8. Comparison between **(A)** the 12 IND (blue) and **(C)** the eight RCS (red) chronologies. Green curves are 40-year low-pass filter. **(B)** Grand average moving 31-year correlations between the 12 IND and eight RCS chronologies computed over their 1040-2011 AD common period, and **(D)** their annual differences (IND minus RCS).

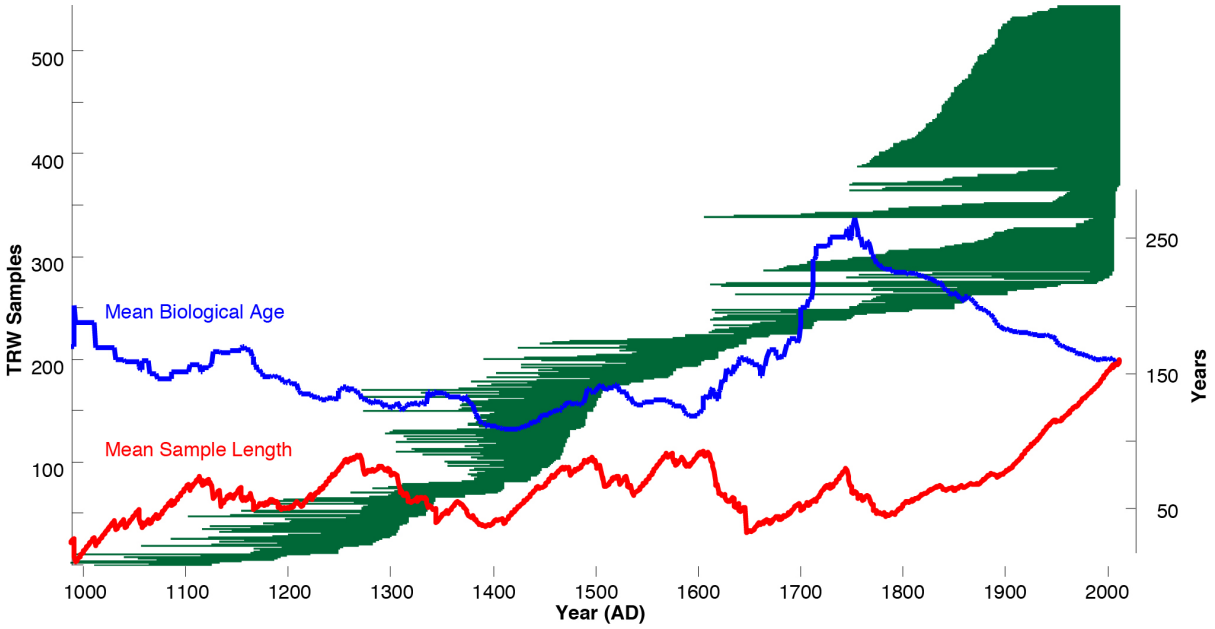

Fig. S9. Temporal distribution of 545 individual TRW samples (green horizontal bars) sorted by their innermost rings, together with the course of mean biological age (MBA; blue) and the mean segment length (MSL; red).

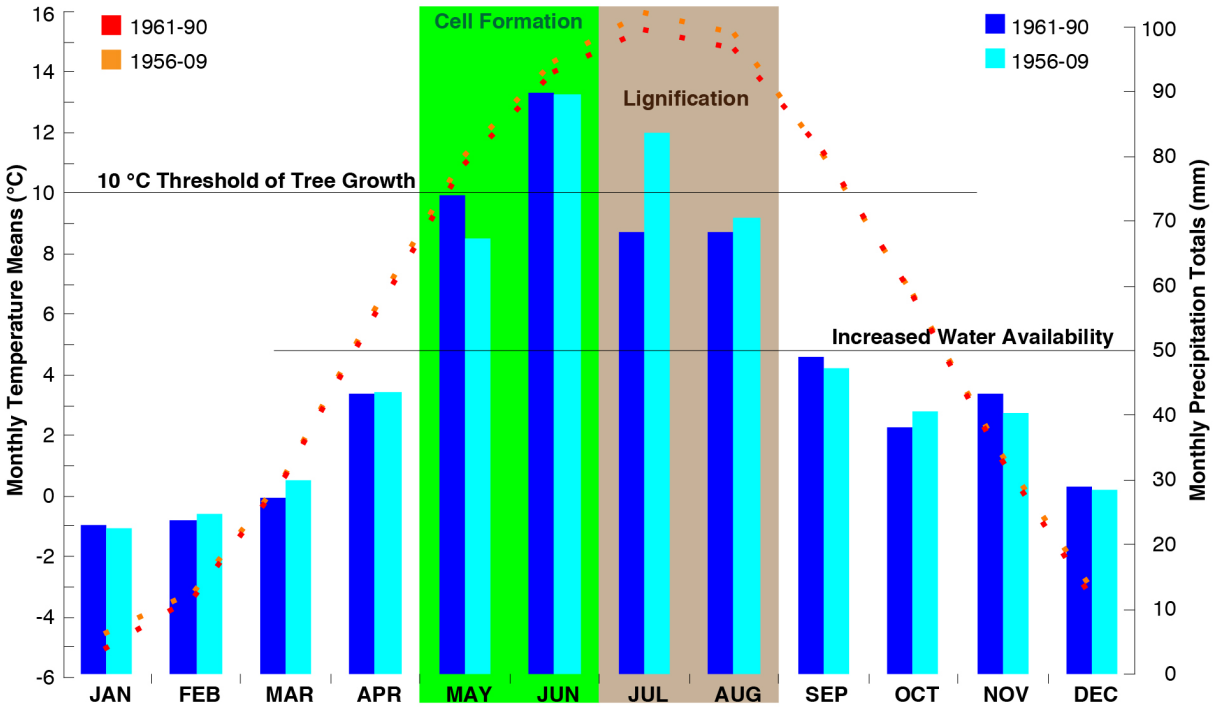

Fig. S10. Monthly resolved climate diagram based on temperature means and precipitation totals from Poprad in northern Slovakia nearby the sampling sites, expressed as means of the 1961-1990 meteorological reference period, and the 1956-2009 proxy/target calibration period. The station (#11934) is located at 49°10'N, 20°30'E, and 709 m asl. Green and brown

shadings refer to those intervals during which presumably cell formation (radial growth) and lignification (cell wall thickening) occurs.

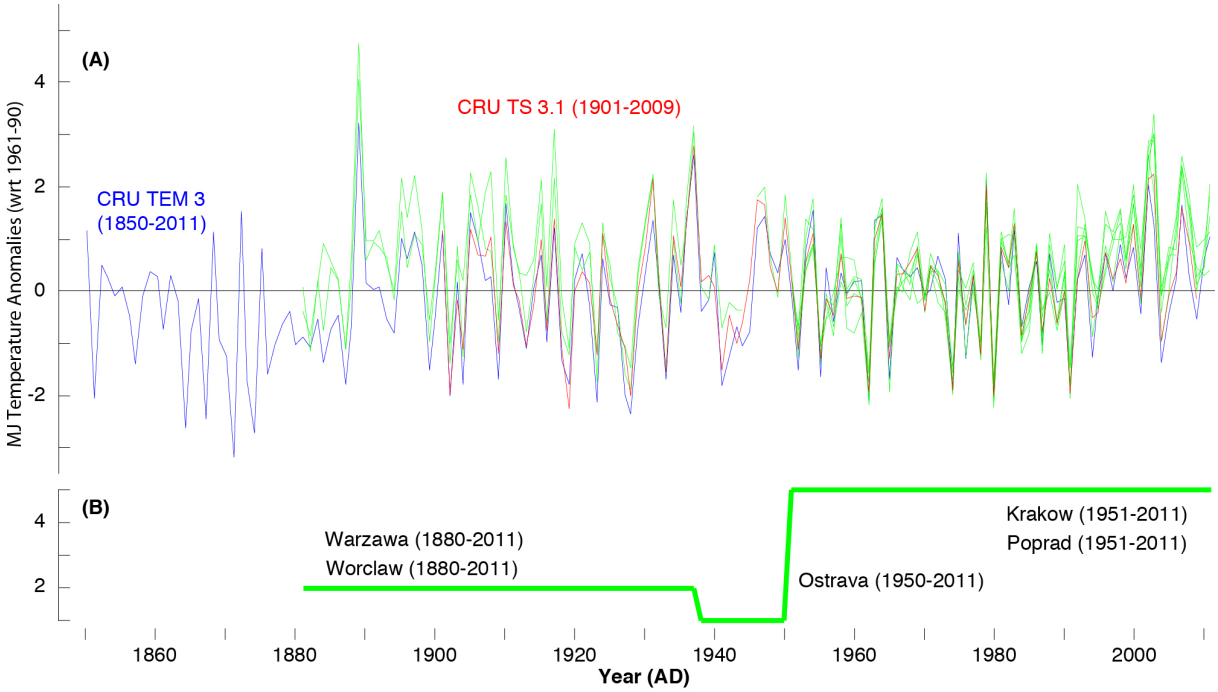

Fig. S11. (A) Variability and **(B)** availability of instrumental station measurements (green) in the greater region of the Tatra Mountains including Slovakia, Poland, Ukraine and the Czech Republic. Additionally interpolated grid-box data are shown in blue (5.0°x5.0°) and red (0.5°x0.5°).

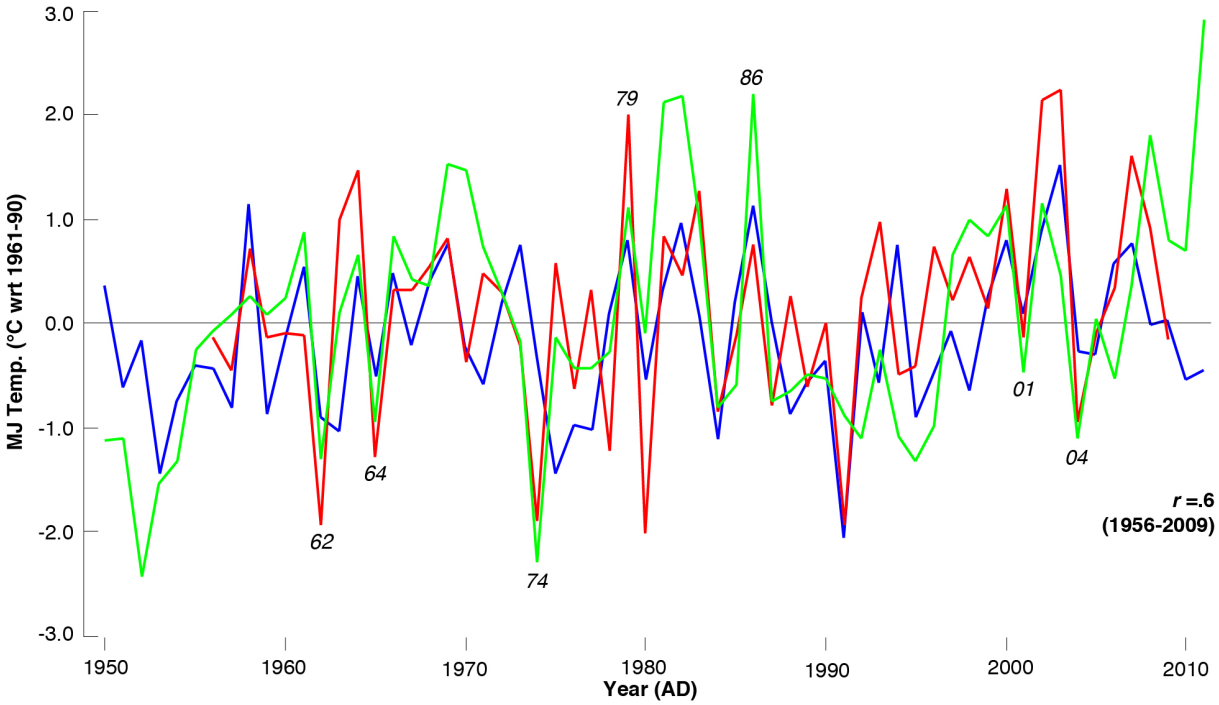

Fig. S12. Measured (red) and reconstructed (green) May-June (MJ) temperature anomalies after scaling over the 1956-2009 period of reliable proxy/target overlap with the common extremes being labeled. Blue curve represents the East Atlantic pattern (EA).

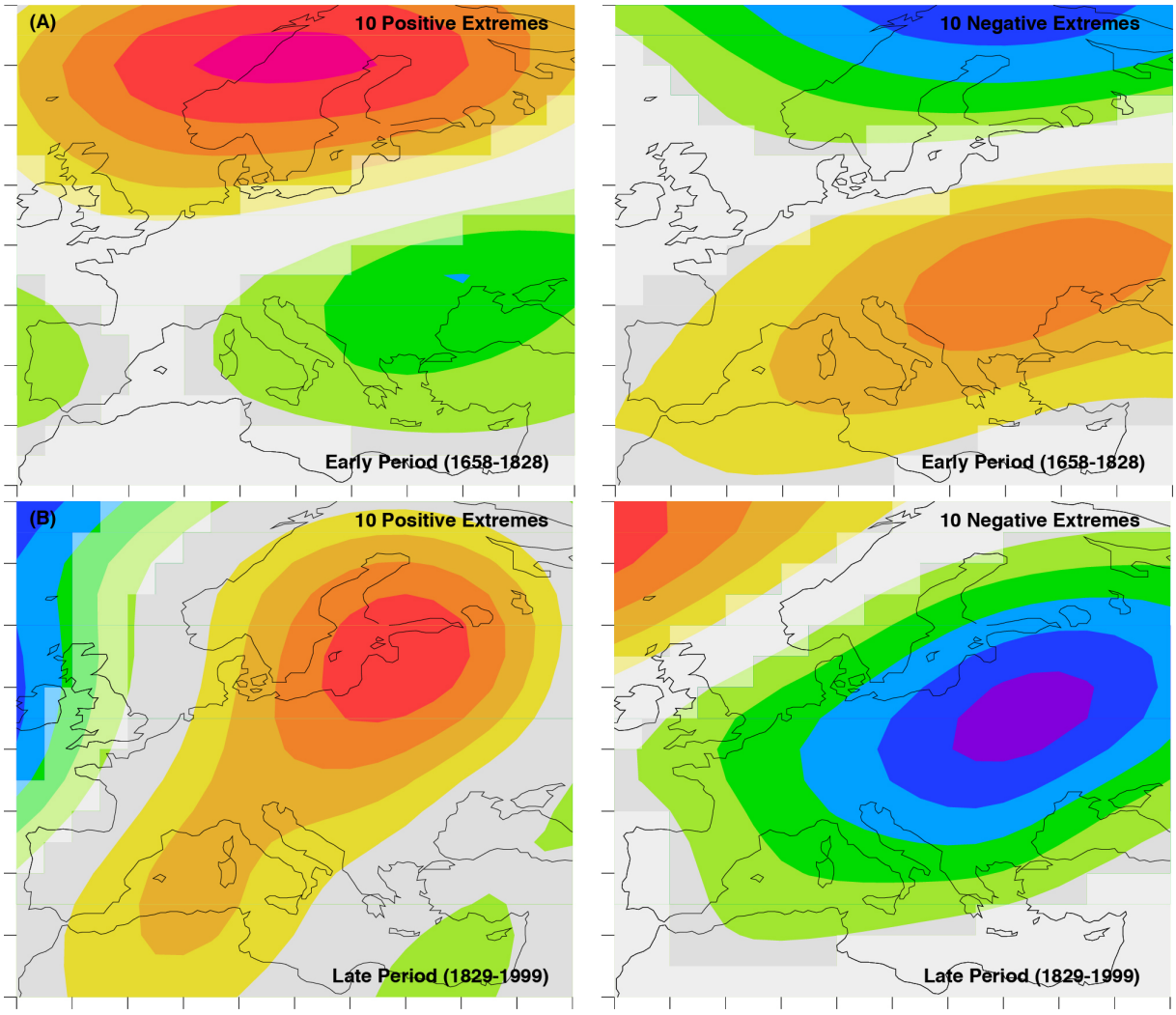

Fig. S13. Composite analysis of the reconstructed 10 most positive/negative (left/right) extremes against MJ 500 hPa geopotential heights (gpm) computed over **(A)** the early 1658-1828 and **(B)** the late 1829-1999 period.

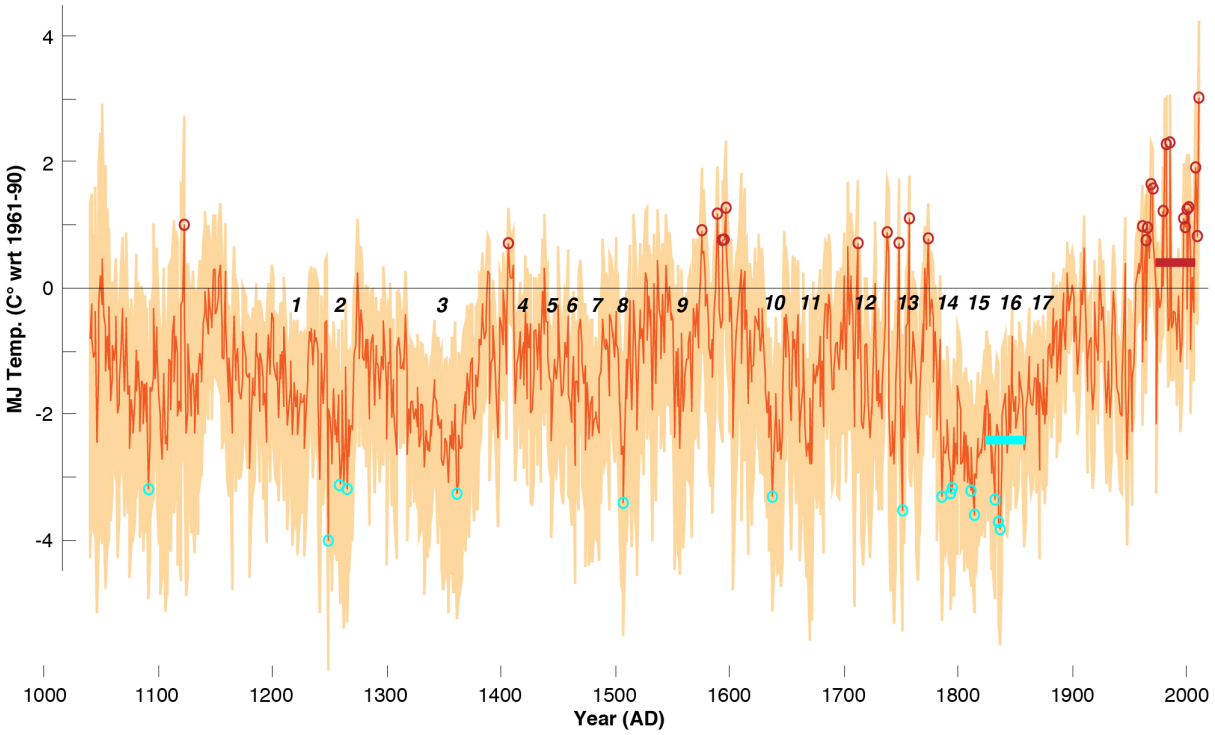

Fig. S14. Reconstructed MJ temperatures (dark orange) and its uncertainty range (orange shading). The red and blue circles refer to the 33 warmest and 16 coldest years (> 2 STDEVs), whereas the horizontal pink and blue bars refer to the warmest (0.3° C) and coldest (-2.45° C) 30-year intervals. Important historical events of Eastern Europe with special emphasis on the Baltic region: 1 = Conquest of Prussia by Teutonic Order, 2 = Mongolian Invasion, 3 = Black Death, 4 = Battle of Grunwald, 5 = Lithuanian Crusade and Polish-Lithuanian Union, 6 = Thirteen Years' War, 7 = Fall of the Golden Horde, 8 = Rise of the Hanseatic League, 9 = Livonian War, 10 = Polish-Muscovite War, 11 = Second Northern War, 12 = Great Northern War, 13 = Seven Years' War, 14 = Partitions of Poland, 15 = French Invasion of Russia, 16 = Polish-Russian War, 17 = January Uprising.

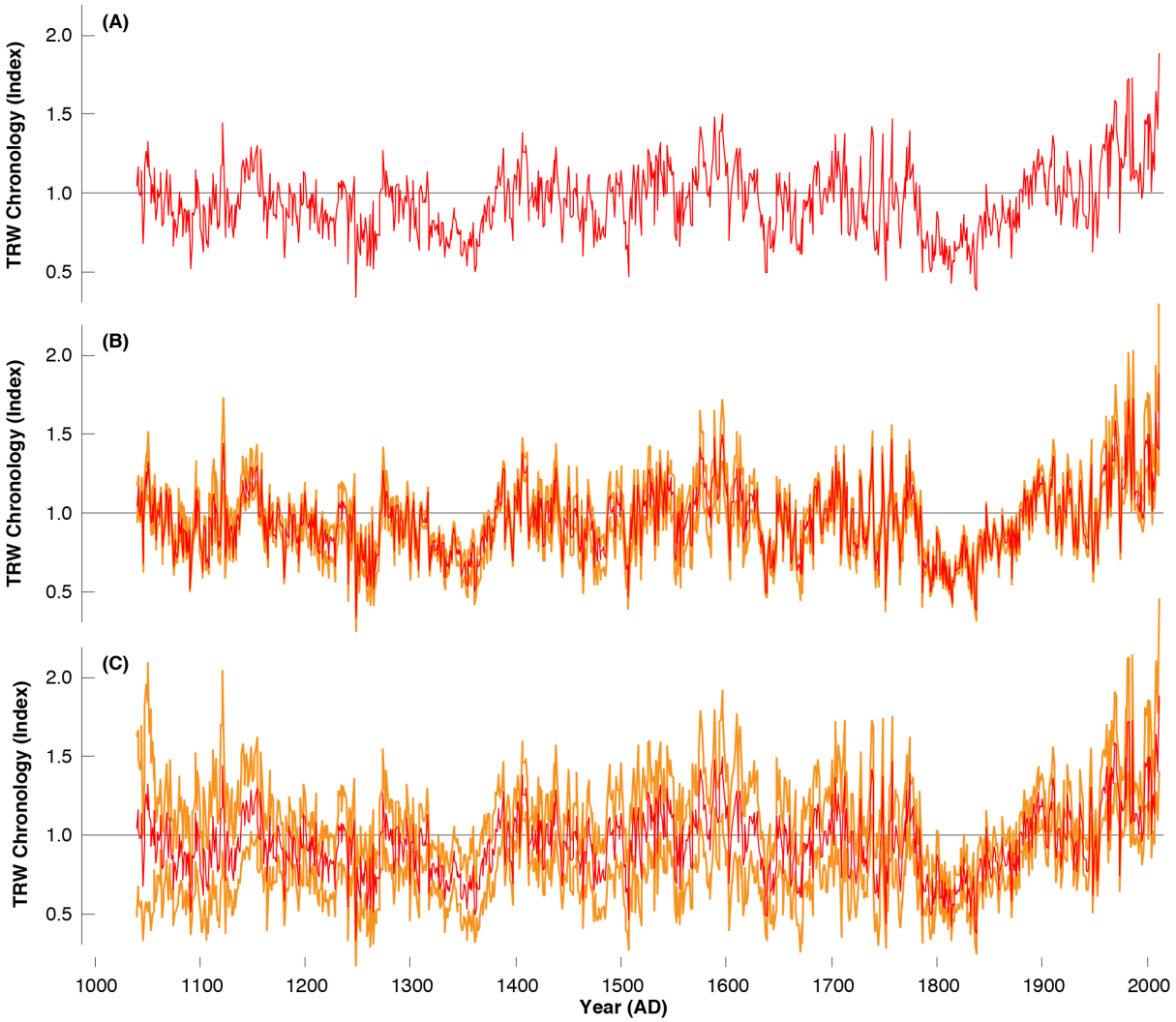

Fig. S15. (A) Mean time-series of the RCS ensemble (red) based on all 545 living and historical larch samples and using eight slightly different chronology development strategies (i.e. All-RCS_10sp, ALL-RCS_67sp, ALL-RCS_PT_10sp, ALL-RCS_PT_67sp, Liv/hist-RCS_10sp, Liv/hist-RCS_67sp, Liv/hist-RCS_PT_10sp, Liv/hist-RCS_PT_67sp). **(B)** Mean time-series of the RCS ensemble (red) together with the uncertainty range (orange) derived from the annual minimum and maximum values of the eight slightly different chronology development strategies. **(C)** Mean time-series of the RCS ensemble (red) together with the combined uncertainty range (orange) derived from the annual minimum and maximum values of the eight slightly different chronology development strategies (as indicated above) and the 95% bootstrap error (obtained from the ARSTAN software). All time-series cover the period 1040-2011 AD during which sample replication constantly ranges >5 cores with a maximum of 271 samples in 1986/1987.

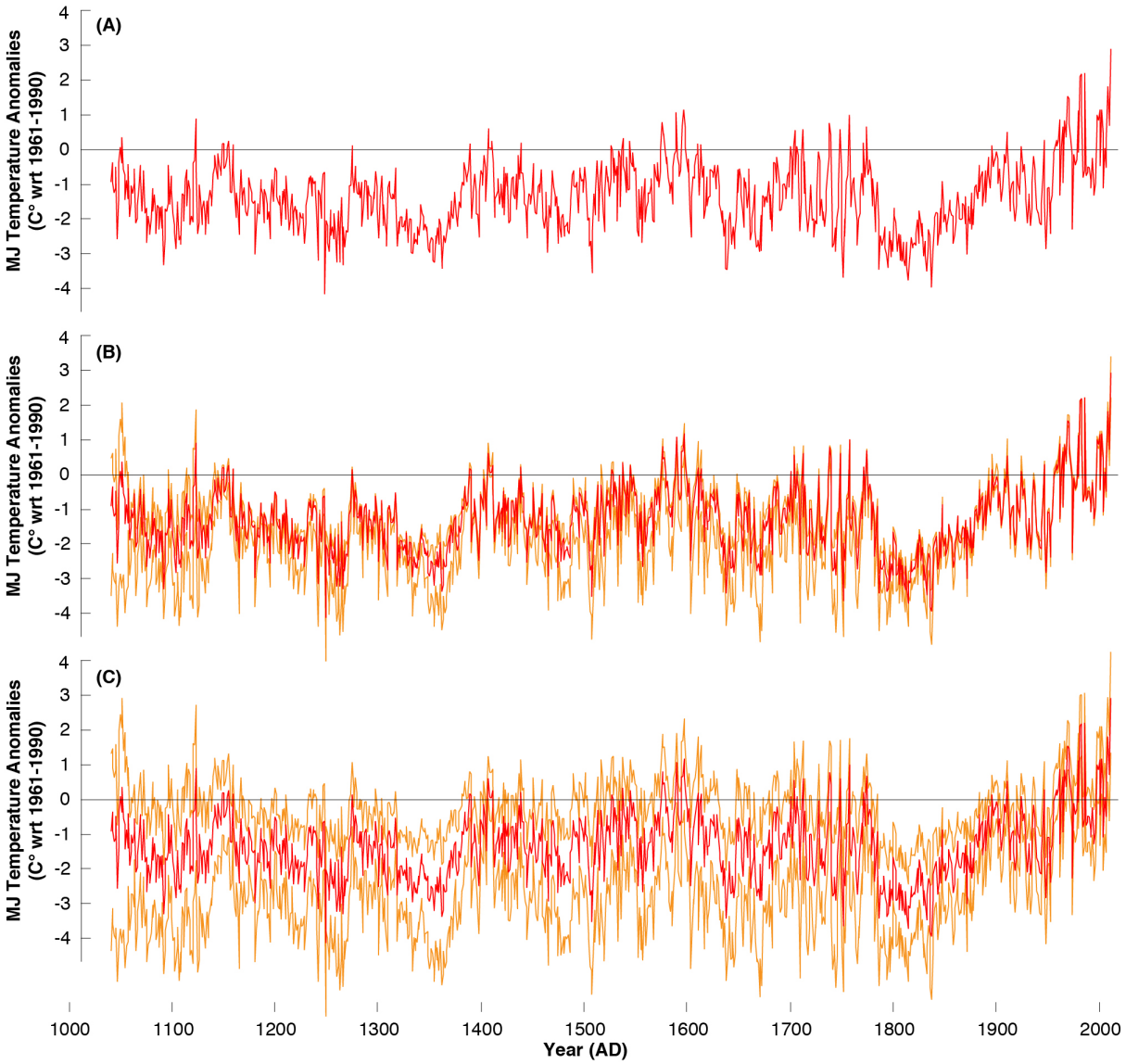

Fig. S16. (A) The final MJ temperature reconstruction (red) of the 1040-2011 period together with **(B)** the (asymmetric) combined data, detrending and chronology error, and **(C)** the (symmetric) calibration error (+/-1 RMSE).

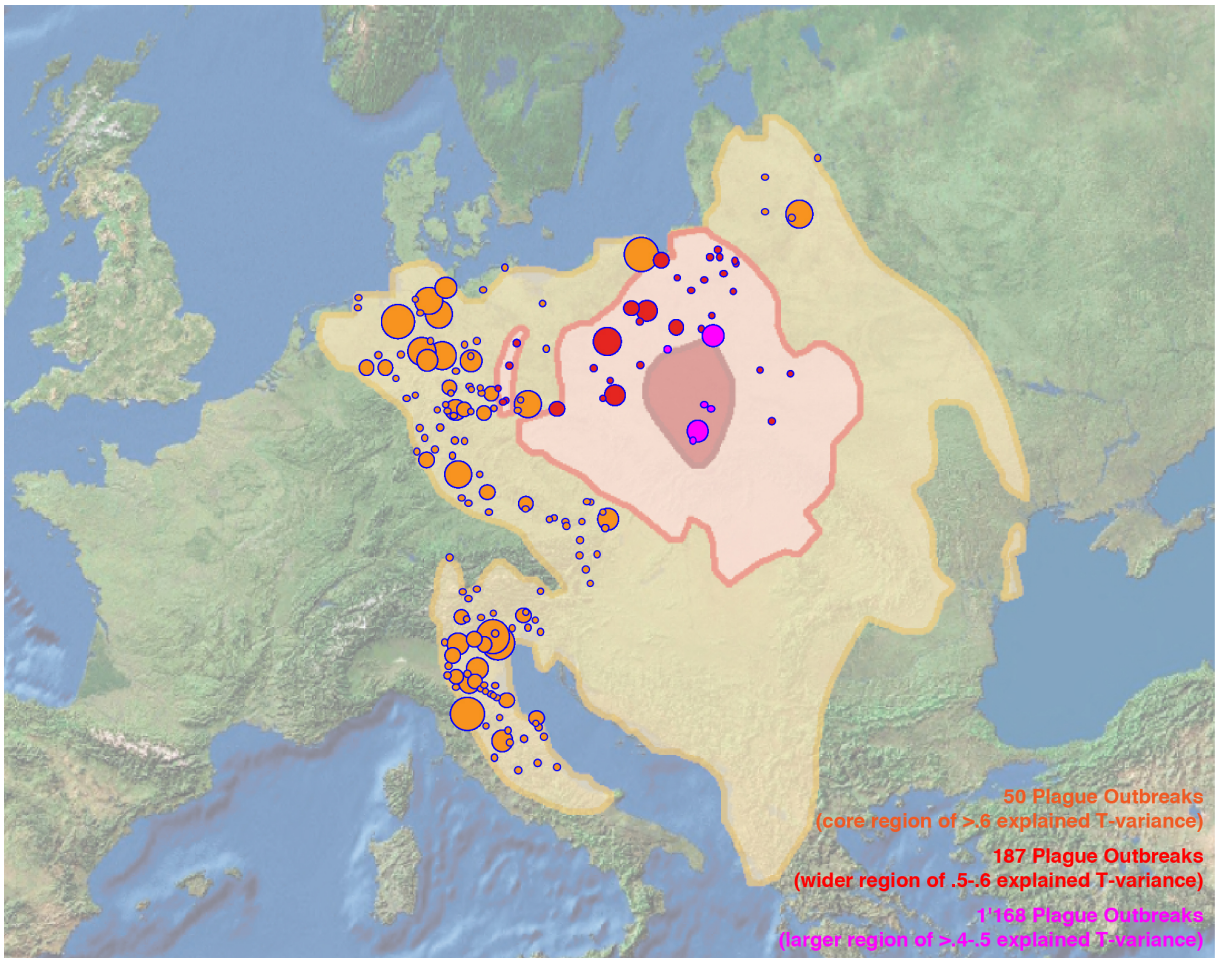

Fig. S17. Spatial distribution of a total of 1'168 plague outbreaks that occurred in the period 1348-1798. Size of the individual circles refers to the amount of events per location, and colors indicate the relative position of the events with respect to the different spatial domains of explained temperature variance.

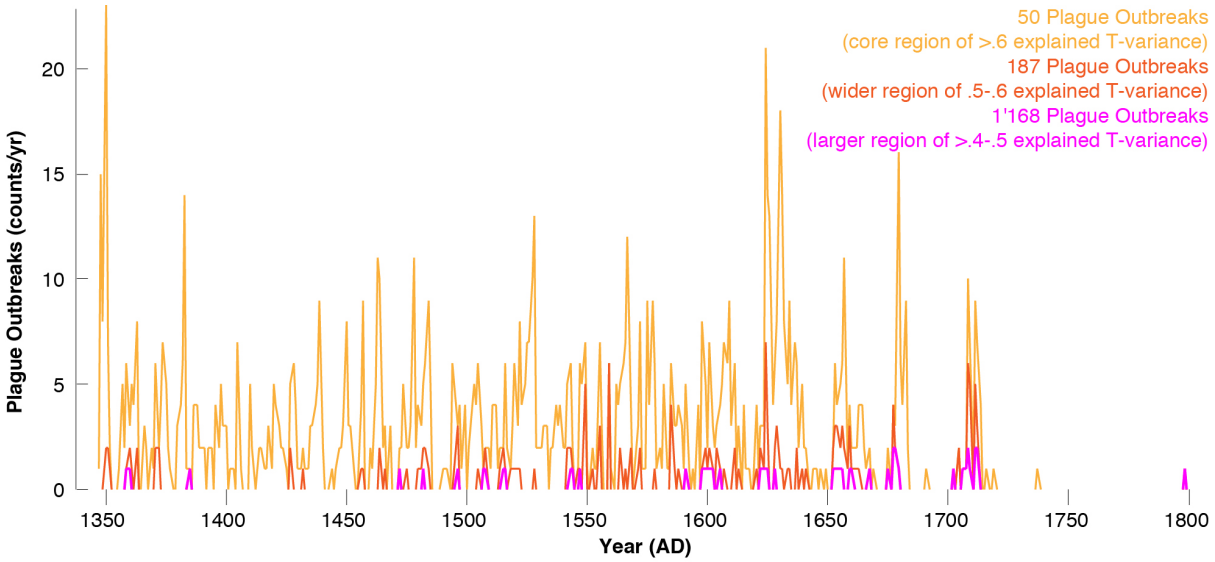

Fig. S18. Temporal distribution of a total of 1'168 plague outbreaks that occurred in the period 1348-1798, herein classified according to their relative position with respect to the different spatial domains of explained temperature variance.

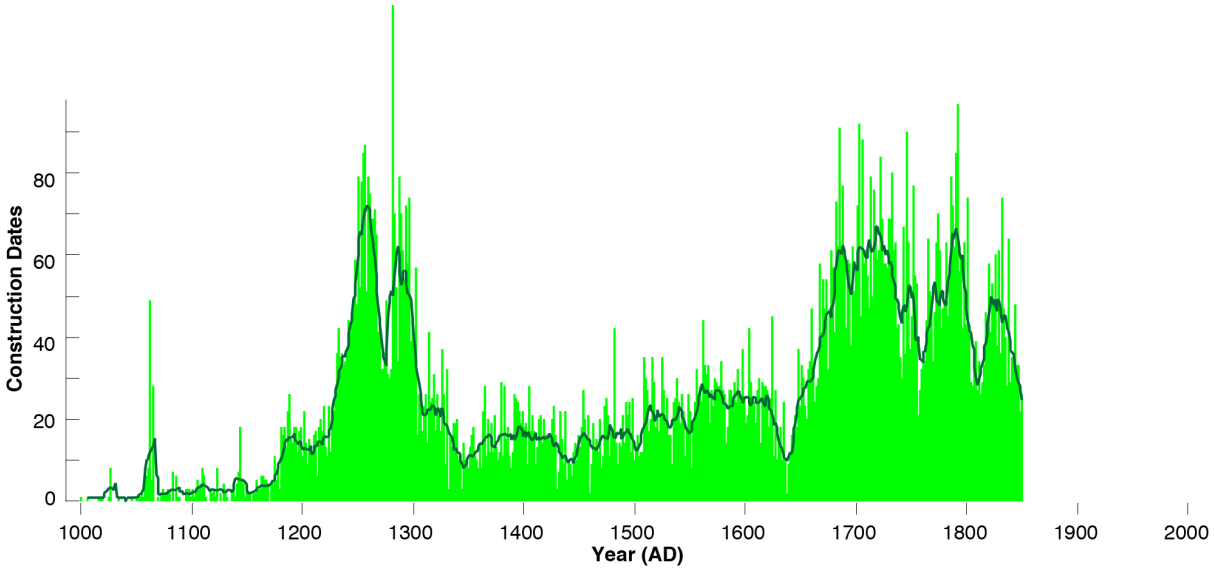

Fig. S19. Temporal distribution of 20,737 regional construction dates between 1000 and 1850 AD. The individual felling dates are accumulated per year (green vertical bars) and for visual evaluation also smoothed (dark green line).